

Cranked Hartree-Fock-Bogoliubov Calculation for Rotating Bose-Einstein Condensates

Nobukuni Hamamoto* and Makito Oi

*Department of Physics, University of Surrey
Guildford, Surrey, GU2 7XH, United Kingdom*

Naoki Onishi

*Department of Information System, Tokyo International University
1-13-1 Matoba-kita, Kawagoe, Saitama, 350-1197, Japan*

(Dated: February 1, 2008)

Abstract

A rotating bosonic many-body system in a harmonic trap is studied with the 3D-Cranked Hartree-Fock-Bogoliubov method at zero temperature, which has been applied to nuclear many-body systems at high spin. This method is a variational method extended from the Hartree-Fock theory, which can treat the pairing correlations in a self-consistent manner. An advantage of this method is that a finite-range interaction between constituent particles can be used in the calculation, unlike the original Gross-Pitaevskii approach. To demonstrate the validity of our method, we present a calculation for a toy model, that is, a rotating system of ten bosonic particles interacting through the repulsive quadrupole-quadrupole interaction in a harmonic trap. It is found that the yrast states, the lowest-energy states for the given total angular momentum, does not correspond to the Bose-Einstein condensate, except a few special cases. One of such cases is a vortex state, which appears when the total angular momentum L is twice the particle number N (i.e., $L = 2N$).

*Present Address, Integrated Information Processing Center, Niigata University
8050 Ikarashi 2-no-cho, Niigata, 950-2181, Japan
; Electronic address: hamamoto@cc.niigata-u.ac.jp

I. INTRODUCTION

Since the Bose-Einstein condensation (BEC) was realized in trapped dilute atomic gases at ultra-low temperature, theoretical studies of the BEC have been rapidly developing.

In the early stage of study, ultra-cold alkali atoms such as ^{87}Rb and ^{23}Na were mainly used for a formation of the BEC. Many theoretical analyses were performed with the Gross-Pitaevskii (GP) equation, in which the two-body interaction takes a delta-function form. In fact, the two-dimensional GP equation is suitable particularly for the study of the BEC made of alkali atoms in a cylindrical trap, where the s-wave scattering is dominant.

Thanks to recent experimental developments, non-alkali atoms and molecules were also cooled down to form the BEC. Such an example is seen in the condensate of Cr atoms [1]. The inter-atomic potential in the BEC made of Cr atoms cannot be approximated exclusively by the delta function because of the strong dipole moment carried by a Cr atom [2, 3]. Therefore, the dipole-dipole interaction (including a tensor force) could be also responsible for the many-body dynamics, which involves the d-wave scattering in the BEC. Another example is the condensate of molecules [4], where the delta function is not appropriate for the intermolecular interaction because of the anisotropic nature of the interaction.

The BEC can be rotated with the state-of-the-art experimental techniques, such as the laser spoon [5]. Owing to these techniques, it was demonstrated that the BEC undergoes the quantum phase transition to vortex states. The “cranked” GP equation was applied to the analysis of the rotating BEC, and it successfully explained the quantum phase transition, including the triangular lattice of vortices [6, 7]. In the early stage of the study of the rotating BEC, the two-dimensional GP equation was mainly used for theoretical analyses [8], because the BEC was only rotated about the fixed axis.

Recently observed phenomena, such as precession [9, 10] and bending [11] of vortices, require the rotational axis to move around in a time-dependent manner, with respect to a certain coordinate frame. These phenomena attract much interest in terms of the three-dimensional spatial structures of the vortex states. Hence, the three-dimensional GP equation is now being applied to various vortex states [12, 13, 14, 15, 16]. In addition, a topological technique was developed to produce vortices with spin 2 or 4 (\hbar), by reversing the magnetic field of the trap [17, 18]. (Below, we take the unit for angular momentum to be $\hbar = 1$.) The formation mechanism of such vortices requires three-dimensional motion of the

vortices. In these situations, the total angular momentum vector needs to be treated in a three-dimensional manner.

In this way, everytime new experimental progresses are achieved, new physical situations are created, to which the original GP equation cannot be applied in a naive way. The cranked Hartree-Fock-Bogoliubov (cranked HFB) method, which has been used to describe rotational states of atomic nuclei [19, 20], could be a useful and powerful approach in order to deal with these new situations.

Rotating BEC systems in a trap has been analyzed with the GP equation, or the exact diagonalization method using a set of the truncated basis. Mottelson was the first to discuss the “yrast” structure [21]. Here, the yrast states mean the lowest-energy states for given angular momentum. He proposed a scenario [22] that the quadrupole excitation is dominant when the total angular momentum L is much less than the particle number N ($L \ll N$), and that all the bosonic particles will occupy the p state when the total angular momentum becomes equal to the particle number. This situation can be interpreted as a creation of a vortex state. This prediction was numerically verified by himself and his collaborators using the two-dimensional GP equation [23]. Bertsch and Papenbrock also verified this prediction using the diagonalization of the two-dimensional model Hamiltonian [25, 26]. Further detailed analysis was performed by Nakajima et. al.[27].

In this paper, we apply the cranked HFB method to a simple schematic model, where bosonic particles interact weakly through the repulsive quadrupole-quadrupole interaction. This model is too simple to describe the detailed structure of realistic systems. But, in limited situations, the quadrupole-quadrupole interaction becomes a phenomenologically valid interaction that can reflect physically essential properties of the realistic interaction. For example, our model can describe low-energy rotational excitations of weakly interacting alkali atoms, as discussed by Mottelson [22]. Then, using the density matrix of the yrast states, as well as its eigenvalues and eigenstates, we compare our results with the other methods. Creation of a vortex state is also discussed within the framework of our model.

In Sections II and III, we present how the cranked HFB theory is extended so as to calculate not only fermionic systems but also bosonic ones. Unlike the GP equation, we do not assume the inter-atomic potential to be the delta function. Also, we do not suppose an *a priori* existence of the condensate, which is the essential assumption in the GP equation. The cranked HFB theory is a constrained mean-field theory, and the value and direction of

the total angular momentum vector are controlled in the calculation. With this method, it is expected that we can numerically analyze not only structure of dilute many-boson systems in a trap, but also superfluidity produced by ultra-cold many-fermion systems in a trap. In the present study, we focus on the study of weakly interacting Bose systems, and an application of the cranked HFB theory to a simple model is presented in Sections IV and V.

II. CRANKED HARTREE-FOCK-BOGOLIUBOV THEORY

We describe the cranked HFB method that can be applied to rotating particles interacting two-body interactions. This method was originally proposed for a description of nuclear rotation [19, 20], but we extend the method to deal with not only fermions but bosons.

Let $c_\alpha^\dagger, c_\alpha$ be the creation and annihilation operators of the single particle state $\langle \xi | \alpha \rangle = \psi_\alpha(\xi)$, where ξ represents the real-space coordinates, spin coordinates and nuclear spin of particles. The creation and annihilation operators of quasi-particle a_i^\dagger, a_i is given by the Bogoliubov-Valatin transformation [28, 29],

$$a_i^\dagger = \sum_\alpha U_{\alpha i} c_\alpha^\dagger + V_{\alpha i} c_\alpha, \quad (1)$$

$$a_i = \sum_\alpha U_{\alpha i}^* c_\alpha + V_{\alpha i}^* c_\alpha^\dagger. \quad (2)$$

The operators a_i, c_α obey the following commutation rule,

$$[a_i, a_j^\dagger]_\pm = \delta_{ij}, \quad [a_i^\dagger, a_j^\dagger]_\pm = [a_i, a_j]_\pm = 0, \quad (3)$$

$$\left[c_\alpha, c_\beta^\dagger \right]_\pm = \delta_{\alpha\beta}, \quad [c_\alpha^\dagger, c_\beta^\dagger]_\pm = [c_\alpha, c_\beta]_\pm = 0,$$

where the upper sign (+) applies to fermions and the lower (−) to bosons. To satisfy the commutation rule (3), we need the following relations.

$$U^\dagger U \pm V^\dagger V = 1, \quad U^T U^* \pm V^T V^* = 1, \quad (4)$$

$$U^\dagger V^* \pm V^\dagger U^* = 0, \quad V^T U \pm U^T V = 0. \quad (5)$$

Based on the variational principle, the U and V are determined. The variational ansatz is chosen to be

$$|\Phi\rangle = N_f \exp\left(\sum_{\alpha\beta} \frac{1}{2} f_{\alpha\beta} c_\alpha^\dagger c_\beta^\dagger\right) |0\rangle, \quad f_{\alpha\beta} = \sum_i V_{\alpha i} (U^{*-1})_{i\beta}, \quad (6)$$

where, N_f is a normalization constant and $|0\rangle$ is the true vacuum. The variational state $|\Phi\rangle$ corresponds to the vacuum in the quasi-particle basis, that is, $a_i|\Phi\rangle = 0$. The many-body Hamiltonian including a two-body interaction $V(\xi_1, \xi_2)$ is generally written as

$$\hat{H} = \sum_{\alpha\beta} H_{\alpha\beta}^0 c_\alpha^\dagger c_\beta + \frac{1}{4} \sum_{\alpha\beta\gamma\delta} \mathcal{V}_{\alpha\beta\gamma\delta} c_\alpha^\dagger c_\beta^\dagger c_\delta c_\gamma, \quad (7)$$

where $\mathcal{V}_{\alpha\beta\gamma\delta}$ is given by

$$\mathcal{V}_{\alpha\beta\gamma\delta} = \langle \psi_\alpha(\xi_1) \psi_\beta(\xi_2) | V(\xi_1, \xi_2) | \psi_\gamma(\xi_1) \psi_\delta(\xi_2) \rangle \mp \langle \psi_\alpha(\xi_1) \psi_\beta(\xi_2) | V(\xi_1, \xi_2) | \psi_\delta(\xi_1) \psi_\gamma(\xi_2) \rangle. \quad (8)$$

The one-body part $H_{\alpha\beta}^0$ includes the kinetic energy and the spherical confinement potential. Using Wick's theorem, we can represent the Hamiltonian (7) by the total energy E and the one-body Hamiltonian \hat{h} , as

$$\hat{H} = E + \hat{h} + \frac{1}{4} \sum_{\alpha\beta\gamma\delta} \mathcal{V}_{\alpha\beta\gamma\delta} : c_\alpha^\dagger c_\beta^\dagger c_\delta c_\gamma :, \quad (9)$$

$$E = \sum_{\alpha\beta} H_{\alpha\beta}^0 \langle c_\alpha^\dagger c_\beta \rangle + \frac{1}{4} \sum_{\alpha\beta\gamma\delta} \mathcal{V}_{\alpha\beta\gamma\delta} (\langle c_\delta c_\gamma \rangle \langle c_\alpha^\dagger c_\beta^\dagger \rangle + \langle c_\alpha^\dagger c_\beta^\dagger \rangle \langle c_\delta c_\gamma \rangle + 2 \langle c_\alpha^\dagger c_\gamma \rangle \langle c_\beta^\dagger c_\delta \rangle), \quad (10)$$

$$\hat{h} = \sum_{\alpha\beta} H_{\alpha\beta}^0 : c_\alpha^\dagger c_\beta : + \frac{1}{4} \sum_{\alpha\beta\gamma\delta} \mathcal{V}_{\alpha\beta\gamma\delta} (\langle c_\delta c_\gamma \rangle : c_\alpha^\dagger c_\beta^\dagger : + \langle c_\alpha^\dagger c_\beta^\dagger \rangle : c_\delta c_\gamma : + 2 \langle c_\alpha^\dagger c_\gamma \rangle : c_\beta^\dagger c_\delta :), \quad (11)$$

where $: \dots :$ is the normal order product with respect to a, a^\dagger and an abbreviated expression is introduced for an expectation value, $\langle \mathcal{O} \rangle = \langle \Phi | \mathcal{O} | \Phi \rangle$.

The HFB wavefunction $|\Phi\rangle$ is determined through the variational principle with constraints \hat{C}_n ,

$$\delta \langle \Phi | \hat{H} - \sum_n \mu_n \hat{C}_n | \Phi \rangle = 0, \quad (12)$$

where μ_n is a Lagrange multiplier. In this method, three components of the total angular momentum and the particle number are constrained. Further constraints are imposed on the following quadrupole operators, $\hat{B}_1 = \sqrt{\frac{15}{2\pi}} yz$, $\hat{B}_2 = \sqrt{\frac{15}{2\pi}} zx$, $\hat{B}_3 = \sqrt{\frac{15}{2\pi}} xy$, in order to fix the intrinsic coordinate axes of the system along the principal axes of the quadrupole moments. Therefore, we have seven constraints in our calculations.

$$\langle \Phi | \hat{J}_x | \Phi \rangle = J_x, \langle \Phi | \hat{J}_y | \Phi \rangle = J_y, \langle \Phi | \hat{J}_z | \Phi \rangle = J_z, \quad (13)$$

$$\langle \Phi | \hat{B}_1 | \Phi \rangle = 0, \langle \Phi | \hat{B}_2 | \Phi \rangle = 0, \langle \Phi | \hat{B}_3 | \Phi \rangle = 0, \quad (14)$$

$$\langle \Phi | \hat{N} | \Phi \rangle = N, \quad (15)$$

In Eq.(12), these constraints are represented with \hat{C}_n 's as $\hat{C}_1 = \hat{J}_x, \hat{C}_2 = \hat{J}_y, \hat{C}_3 = \hat{J}_z, \hat{C}_4 = \hat{B}_1, \hat{C}_5 = \hat{B}_2, \hat{C}_6 = \hat{B}_3, \hat{C}_7 = \hat{N}$. In particular, the term $-\sum_{n=1}^3 \mu_n \hat{C}_n$ has been called the “cranking term” in nuclear high-spin physics, because it simulates the effect of the Coriolis force in the rotating mean-field system.

III. METHOD OF STEEPEST DESCENT

As mentioned earlier, we determine the HFB states, following the variational principle. By multiplying a unitary operator to an arbitrary initial HFB state $|\Phi\rangle$, another HFB state $|\Phi'\rangle$ is obtained. This transformation is considered as a variational procedure with respect to the matrices U and V of the Bogoliubov-Valatin transformation, Eq.(2). The transformation is iterated until a local minimum is found to satisfy Eq.(12).

Now, let us explain how the unitary operator is given within our framework. First of all, from the extended Thouless theorem [30, 31], the unitary transformation of the HFB state is expressed as

$$|\Phi'\rangle = \exp(\hat{d})|\Phi\rangle, \quad (16)$$

where \hat{d} is an anti-Hermitian operator $\hat{d} = -\hat{d}^\dagger$, which is generally expressed as,

$$\hat{d} = \frac{1}{2} \sum_{ij} \left(d_{ij} a_i^\dagger a_j^\dagger - d_{ij}^* a_j a_i \right). \quad (17)$$

A quasi-particle basis is then transformed in the following way.

$$\begin{pmatrix} a_i'^\dagger \\ a_i' \end{pmatrix} = \begin{pmatrix} e^{-\hat{d}} a_i^\dagger e^{\hat{d}} \\ e^{-\hat{d}} a_i e^{\hat{d}} \end{pmatrix} = \exp(\pm \mathcal{D})^T \begin{pmatrix} a_i^\dagger \\ a_i \end{pmatrix}, \quad (18)$$

where

$$\mathcal{D} = \begin{pmatrix} 0 & d \\ d^* & 0 \end{pmatrix}, \quad (19)$$

and d is a matrix representation of \hat{d} . We choose the anti-Hermite operator \hat{d} as,

$$\hat{d} = [\eta \hat{r} + \hat{s}]^a, \quad (20)$$

where we define $[\hat{O}]^a = \frac{1}{2} [\hat{\mathcal{N}}, \hat{O}]$ and the quasi-particle number operator is given as $\hat{\mathcal{N}} =$

$\sum_i a_i^\dagger a_i$. An operator \hat{s} and the single-particle Routhian \hat{r} are respectively defined as

$$\hat{s} = \sum_n \delta_n \hat{C}_n, \quad (21)$$

$$\hat{r} = \hat{h} - \sum_n \mu_n \hat{C}_n. \quad (22)$$

Then, these parameters η , δ_n , and μ_n are determined through a minimization of $\langle \Phi' | \hat{H} | \Phi' \rangle$ under the constraints $\langle \Phi | \hat{C}_i | \Phi \rangle = c_i$. The parameters δ_n and μ_n are evaluated by expanding $\langle \Phi' | \hat{C}_i | \Phi' \rangle$ up to the first order in δ_n and μ_n . That is,

$$\delta_k = \sum_i L_{ki}^{-1} (c_i - \langle \Phi | \hat{C}_i | \Phi \rangle), \quad (23)$$

$$\mu_k = \sum_i L_{ki}^{-1} \langle \Phi | [\hat{C}_i, [\hat{h}]^a] | \Phi \rangle, \quad (24)$$

where $L_{ki} = \langle \Phi | [\hat{C}_i, [\hat{C}_k]^a] | \Phi \rangle$. Whereas, the parameter η is determined from a minimization condition for $E = \langle \Phi' | \hat{H} | \Phi' \rangle$, through expanding E up to the second order in η . As a consequence, we have

$$\eta = - \frac{\langle \Phi | [\hat{H}, [\hat{r}]^a] | \Phi \rangle + \langle \Phi | [[\hat{H}, [\hat{r}]^a], [\hat{s}]^a] | \Phi \rangle}{\langle \Phi | [[\hat{H}, [\hat{r}]^a], [\hat{r}]^a] | \Phi \rangle}. \quad (25)$$

To check the convergence for the self-consistency in the calculation, it is convenient to define the norm of d as $|d| = \sqrt{\sum_{ij} \frac{1}{2} |d_{ij}|^2}$. In our calculations, a criterion for the convergence is given whether $|d|$ is less or greater than $\epsilon = 1.0 \times 10^{-7}$. When $|d| < \epsilon$, we judge that the convergence is numerically achieved. Otherwise, the iteration for the self-consistency continue until $|d|$ meets the above condition.

IV. A SCHEMATIC MODEL

To examine the convergence procedure of our method (3D-cranked HFB) for the bosonic case, let us consider a toy model, which is similar to a realistic system of dilute ultra-cold Bose gases confined by an isotropic harmonic oscillator potential $V(r) = \frac{1}{2} M \omega^2 r^2$, where M represents the atomic mass. We choose the single-particle states to be the harmonic oscillator states, $\langle \mathbf{r} | \alpha \rangle = \langle \mathbf{r} | c_\alpha^\dagger | 0 \rangle = R_{n_\alpha l_\alpha}(r) i^{l_\alpha} Y_{l_\alpha m_\alpha}(\theta \phi)$, that is, a product of the Laguerre polynomial and the spherical harmonics. Let us denote this basis as $\alpha \equiv (n_\alpha, l_\alpha, m_\alpha)$.

Mottelson discussed that the quadrupole correlation is important in the low angular momentum region [22]. In accordance with his proposition, the following Hamiltonian is

considered in our calculations.

$$\hat{H}_{\text{model}} = \hat{H}_0 + \frac{1}{2}\kappa \sum_{\mu=-2}^2 (-)^{\mu} \hat{Q}_{-\mu} \hat{Q}_{\mu} + g \hat{P}^{\dagger} \hat{P}, \quad (26)$$

$$\hat{H}_0 = \sum_{\alpha} (2n_{\alpha} + l_{\alpha} + \frac{3}{2}) \hbar\omega \delta c_{\alpha}^{\dagger} c_{\alpha}, \quad (27)$$

$$\hat{Q}_{\mu} = \sum_{\alpha\beta} \langle \alpha | 2r^2 C_{\mu}^{(2)} | \beta \rangle c_{\alpha}^{\dagger} c_{\beta}, \quad (28)$$

$$\hat{P} = \sum_{\alpha} \sqrt{2l_{\alpha} + 1} \langle l_{\alpha} m_{\alpha} l_{\alpha} - m_{\alpha} | 00 \rangle c_{\bar{\alpha}} c_{\alpha}, \quad (29)$$

where $c_{\bar{\alpha}}$ is the annihilation operator corresponding to the state $\bar{\alpha} = (n_{\alpha}, l_{\alpha}, -m_{\alpha})$, and $C_{\kappa}^{(k)}(\Omega)$ is related to the spherical harmonics through $C_{\kappa}^{(k)}(\Omega) = \sqrt{\frac{4\pi}{2k+1}} Y_{k\kappa}(\Omega)$. This Hamiltonian should be considered as a simple model for weakly interacting dilute atomic gases. The parameter κ represents strength of the quadrupole-quadrupole interaction, and κ is positive in this work, to treat the repulsive two-body interaction. The last term of Eq. (26) is called the pairing interaction. [24] The parameter g represents the strength of the pairing interaction. In the present calculation, we set g to be zero, for the sake of simplicity. The one-body Hamiltonian (11) in this model is given as,

$$\hat{h}_{\text{model}} = \hat{H}_0 + \kappa \sum_{\mu} (-)^{\mu} \langle \hat{Q}_{-\mu} \rangle \hat{Q}_{\mu} + g \langle \hat{P}^{\dagger} \rangle \hat{P}. \quad (30)$$

The oscillator energy for the isotropic harmonic oscillator states, $\hbar\omega$, is set to 1.9 (meV). The quadrupole-quadrupole interaction κ/A^2 is repulsive and its strength is set to 0.1, 0.5 and 1.0 (meV/ μm^4), where A is the mass number of an atom. The single-particle model space used in this calculation are the harmonic oscillator states of the 0s, 1s, 0d, 2s, 1d, 0g, 0p, 1p, 0f, 2p, 1f and 0h states.

To prepare the initial state, we use the deformed quadrupole mean field.

$$\hat{h}_{\text{deform}} = \hat{H}_0 - \frac{2}{3} M \omega^2 r^2 \left(\beta \cos \gamma C_0^{(2)}(\Omega) + \frac{1}{\sqrt{2}} \beta \sin \gamma (C_2^{(2)}(\Omega) + C_{-2}^{(2)}(\Omega)) \right). \quad (31)$$

The quadrupole parameters (β, γ) are useful measures to think about the shape of the many-body system. β is a measure for elongation or stretching, while γ for triaxiality or deviation from axial symmetry. For example, a spherical shape has $\beta = 0$ and nuclear superdeformation has typically $\beta \simeq 0.6$. The triaxial parameter γ gives axial shapes when $\gamma = 0^\circ$ and $\gamma = 60^\circ$. The former shape corresponds to the so-called “prolate” shape, which

is similar to a kiwifruit, while the latter to “oblate” shape, similar to a mandarin orange. By definition, a triaxial shape is invariant with respect to an operation: $\gamma \rightarrow \gamma + 120^\circ$.

We diagonalize the Hamiltonian (31) for $(\beta, \gamma) = (0.01, 0)$ and obtain the single-particle states. The initial state is created as a Hartree-Fock state, that is, all the single-particle levels are occupied below the Fermi level.

Since the initial state is symmetric under rotation about the z -axis, collective rotation about the z -axis is suppressed. In other words, we cannot crank the state around the symmetry axis. To induce angular momentum, we initially set the constraints of the total angular momentum to $(J_x, J_y, J_z) = (0.05, 0, 0)$. As a next step, we tilt the angular momentum vector to $(J_x, J_y, J_z) = (0, 0, 0.1)$. With this procedure, we can increase J_z up to 20, with a step, $\Delta J_z = 0.05$.

V. RESULTS AND DISCUSSIONS

Figure 1 represents the total energy E as a function of the total angular momentum L . Four lines are plotted in this figure. One dotted line represents $\hbar\omega(L + \frac{3}{2}N)$ and the other three lines are calculated with the different quadrupole-quadrupole interaction strengths, which are $\kappa/A^2 = 0.1, 0.5$ and 1.0 (meV/ μm^4). Despite the different values for κ , These lines are nearly identical. In other words, E is almost independent of κ .

We also find that E increases almost in proportion to L , that is, $E \propto L$. This result can be explained from a microscopic point of view. As L is increased, single-particle excitations are induced one by one through the two-body interaction, so as to satisfy the angular momentum constraints. In other words, $\Delta E = \hbar\omega\Delta L$, where $\hbar\omega$ is the single-particle energy spacing of the isotropic harmonic oscillator. Due to the quantum statistics for bosons, this excitation mode can continue until the number of particles occupying the ground state becomes zero. This linear behavior is already noticed by other authors [25]. However, with a careful look at our numerical result, there is a slight deviation from the linearity in the the total energy ($\hbar\omega(L + \frac{3}{2}N)$). This small deviation is caused by deformation of the mean field, which has a role to mix the single-particle orbits. The evolution of the quadrupole deformation in response to rotation is discussed below.

Figure 2 shows the deformation parameters β and γ . The strengths of the interaction are set in the same manner as in Figure 1. These deformation parameters are self-consistently

calculated as

$$\beta = \frac{3\kappa}{M\omega^2} \sqrt{\langle Q_{20} \rangle^2 + 2\langle Q_{22} \rangle^2}, \quad (32)$$

$$\gamma = \tan^{-1} \frac{\langle Q_{22} \rangle}{\sqrt{2}\langle Q_{20} \rangle}. \quad (33)$$

The unit for the quadrupole moment ($M\omega^2/\kappa$) is derived from the consistency at $L = 0$ between the one-body Hamiltonian (30) and the deformed mean-field Hamiltonian (31). The figure shows that the deformation parameters do not depend on the interaction strength very much, although γ shows minor differences at low spin. When the total angular momentum is small ($L \lesssim 1$), the mean field has a almost spherical shape. This is because the trapping potential is spherical and the present two-body interaction is repulsive. As L is increased, β increases gradually. In the small angular momentum region ($L < 5$), γ is not 180° ($\equiv 60^\circ$). (See the right panel of Figure 2.) This result means that the shape of the mean field is not axial-symmetric, but triaxial. When the quadrupole-quadrupole interaction becomes stronger, the deformation tends to prefer a more triaxial-deformed shape. However, any of the three cases ends up with the oblate shape ($\gamma = 180^\circ$) at high angular momentum ($L \gtrsim 5$). A reason for this tendency can be explained as the following: When the quadrupole-quadrupole interaction is strong, the harmonic oscillator states having the different magnetic quantum numbers become more mixed through the interaction. As a result, the magnetic quantum number is no longer a good quantum number. This is nothing but axial symmetry breaking, or an emergence of triaxiality. It should be noted, however, that γ is substantial only at low angular momentum, where β is very small. In other words, when the elongation is small ($\beta \simeq 0$), the triaxial degree of freedom is irrelevant in terms of a deviation from a spherical shape. That is, in our calculation, the shape of the mean field can be regarded to be almost spherical in the small L region. On the other hand, for the higher angular momentum region ($L > 5$), γ is almost constant to be 180° , meaning that the mean field becomes an oblate shape.

The condition for the BEC of weakly interacting bosonic atoms in a trap is given by $Nv/\hbar\omega \ll 1$ [22], where v is an expectation value of the two-body interaction, while $\hbar\omega$ represents the single-particle level spacing. In our calculation, Nv corresponds to an expectation value of the quadrupole-quadrupole force, that is, $\kappa(\langle Q_{20} \rangle^2 + 2\langle Q_{22} \rangle^2)$. The ratio $Nv/\hbar\omega$ is then estimated to be $4.4 \times 10^{-3} \beta A^2/\kappa$. According to our calculation, deformation is up to $\beta \lesssim 1$, so that the ratio is of order of 10^{-4} to 10^{-5} for our three choices of the

interaction strength ($\kappa/A^2 = 0.1, 0.5, 1 \text{ meV}/\mu\text{m}^4$). This result means that our calculations can be regarded as a weakly interacting many-boson system.

Figure 3 shows the occupation probability, $\rho_{\alpha\alpha}$ for $\kappa/A^2 = 0.1 \text{ meV}/\mu\text{m}^4$, where $\rho_{\alpha\beta}$ is the density matrix defined as

$$\rho_{\alpha\beta} = \sum_i V_{\alpha i}^* V_{\beta i}. \quad (34)$$

(V is a matrix appearing in the Bogoliubov-Valatin transformation, Eq.(2).) Although the occupation probabilities for $\kappa/A^2 = 0.5, 1 \text{ meV}/\mu\text{m}^4$ are not plotted in Figure 3, we have calculated these occupation probabilities and found that they are almost same as that of $\kappa/A^2 = 0.1 \text{ meV}/\mu\text{m}^4$. This result indicates that the wave-function does not strongly depend on the strength of the quadrupole-quadrupole interaction.

At low L , the $(0s0)$ states are the major component in the HFB state. The higher the total angular momentum, the more the $(0d2)$ state admixes with the $(0s0)$ state. The $(0g2)$ component is also mixed at $L \simeq 2N = 20$, while the $(0s0)$ component vanishes. This result suggests that the yrast state changes its structure gradually.

Figure 4 shows the eigenvalue ν_a of the density matrix $\rho_{\alpha\beta}$, as a function of L . Only the plot for $\kappa/A^2 = 0.1 \text{ (meV}/\mu\text{m}^4)$ is displayed because the occupation is almost independent of κ/A^2 . The largest eigenvalue in the figure is equal to the total particle number $N = 10$, and this situation happens only at $L = 0$ and $2N (= 20)$. In these cases, all the particles occupy only one single-particle state, which can be regarded as the condensate state. On the other hand, between $L = 0$ and $2N$ ($0 < L < 2N = 20$), the particles are shared by the two states ψ^A and ψ^B , where $\nu_A + \nu_B = N = 10$. This result indicates that most of the yrast states are non-condensates, but a mixture of two single-particle components, ψ^A and ψ^B .

In Figure 5, the eigenstates ψ^A and ψ^B are decomposed into the single-particle basis, and their components are displayed in terms of probability $(v_\alpha^a)^2$, where $|\psi^a\rangle = \sum_\alpha v_\alpha^a |\alpha\rangle$. First, as shown in the right panel of the figure, the state ψ^A at $L = 0$ is found to have a condensate structure into the $(0s0)$ state, which is consistent with the occupation number calculation shown in Figure 3. As L is increased, the $(0d0)$ component starts to mix with the s component although the contribution from the d state is minor. This mixture is consistent with the growth of the quadrupole deformation, as shown in the left panel of Figure 2. When $L \lesssim 5$, axial symmetry is broken around the cranking axis, as shown in Figure 2. In this situation, the whole system rotates in a collective manner, which is

consistent with Mottelson's model claiming that the yrast structure is dominated by the collective quadrupole excitation at low L . Such a collective rotation was actually observed experimentally at lower rotational frequency before vortices are formed [32]. However, the linear dependence of E on L at low L seen in Figure 1 implies that the collective mode is not the major mode in our model, but that the single-particle excitations are. Next, in the right panel of Figure 5, the state ψ^B is decomposed into the d and g states. This is because the quadrupole-quadrupole interaction does not mix the states having different parity, so that the particles in the s state can not be excited to the p state, but the d or g states. The major component is the $(0d2)$ state when angular momentum is small ($L \lesssim 10$), whereas the $(0g2)$ state starts to mix in the high angular momentum region ($L > 10$), due to the onset of deformation in the mean field. Although the $(0g4)$ state is included already at $L \simeq 0$, this component can be considered as a minor component because the occupation ν_B is nearly 0 in this region.

According to the previous discussion, at $L = 2N$, the many-body state goes into the condensate in the state ψ^B , which is a mixture of the $(0d2)$ and $(0g2)$ states. Both of these $(0d2)$ and $(0g2)$ states have angular dependence $\sin^2 \theta$, so that the density along the z -axis vanishes for these states. Therefore, the condensate at $L = 2N$ is considered as a quantized vortex state carrying 2 (\hbar).

The HFB solutions obtained for the intermediate L values ($0 < L < 20$) are quite different from the solutions obtained with the GP equation. This is because the GP equation assumes an *a priori* existence of the condensate for the whole range of L , which can be expressed as a Hartree state, $(a_0^\dagger)^N |0\rangle$. Although our HFB ansatz includes this condensate state as a special case, the mathematical form for the HFB state is generally more complicated to allow a linear combination form of multiple Hartree states, in accordance with Eq. (6). If the condensate is realized at any L , all the particles should occupy the one single-particle state that is generally expressed by a liner combination of the basis states, such as the s , d and g states.

As shown in Figure 4, the yrast structure changes smoothly from the ψ^A -dominant states to the ψ^B -dominant state, as L is increased from 0 to $2N$. Considering that the latter state at $L = 2N$ corresponds to a vortex state, a formation of the vortex starts as a shallow dent in the center at small L . As the amplitude of ψ^B becomes larger for increasing L , the depth of the dent becomes deeper. Finally at $L = 2N$, a complete vortex is formed, where density

becomes zero. This mechanism of the vortex formation is very different from the one derived from the GP equation. In the calculations using the GP equation [6], a vortex enters from the “outside” of the system due to a continuity of the many-body wave function. This sort of process needs odd-number multipolarities, such as a dipole ($\lambda = 1$) and an octupole ($\lambda = 3$) correlations, which are missing from our present model.

These higher multipole correlations may play an important role also in a formation of vortex lattices, which violates rotational symmetry of the system. In the present framework, vortices appear always in the center of the system due to the axial symmetry possessed by the system. To allow multiple vortices to appear away from the center, we need, at least, a mixing between these states of $(0s0)$, $(0d2)$ and $(0g2)$ to break the symmetry. This situation is realized only when $\langle Q_{2\pm 2} \rangle$, which is contained in the single-particle Hamiltonian, Eq.(30), is non-zero. In other words, the deformation parameter γ should not be equal to 0° or 180° to allow triaxial deformation bringing anisotropy to the system. However, in the present calculations, γ takes the value of 180° in a wide range of angular momentum ($5 < L < 20$). Consequently, the vortex lattice is not produced in our model.

VI. SUMMARY

Extending the 3D-cranked Hartree-Fock-Bogoliubov method, we have performed the numerical calculation for a rotating many-boson system interacting through a weak and repulsive interaction, trapped inside an isotropic harmonic oscillator potential. Unlike the Gross-Pitaevskii equation, our calculation does not assume the existence of the condensate *a priori*, but general many-body states in the framework of the HFB method.

We applied the method to a simple model where the two-body interaction is chosen to be a separable type called the quadrupole-quadrupole interaction. Parity is conserved for this interaction, so that only $\Delta l = 2$ excitations are allowed through the quadrupole-quadrupole interaction.

First of all, at $L = 0$, our calculation shows that the HFB state is interpreted as a condensate into $(0s0)$.

As increasing the total angular momentum L from 0 to 20, the particles in the yrast state transfer from ϕ^A to ϕ^B , which have the magnetic quantum numbers $M_z = 0$ and $M_z = 2$, respectively. At low L , triaxial deformation is formed to allow collective rotation around the

cranking axis. However, the linearity $E \propto L$ implies that the major excitation mode is still single-particle excitations. At higher L , the system becomes oblate, that is, axial symmetric around the rotating axis. Angular momentum is thus produced by migrating from s state to d state. These single-particle excitations are induced from the s to the d state through the quadrupole-quadrupole interaction, in agreement with the prediction by Mottelson.

Finally, at $L = 2N$, the HFB state becomes another condensate, in which all the particles occupy the single state expressed by a linear combination of the $(0d2)$ and $(0g2)$ states. This state can be interpreted as a vortex state having angular momentum $2(\hbar)$.

In this way, the yrast structure changes gradually and smoothly in our framework. This result can be accounted by the following two effects: One is our choice of the HFB ansatz which allows a linear combination form of multiple Hartree states. The other is the finite-number effect of the total particle number ($N = 10$). These effects surely needs further investigations in the future studies.

We are currently proceeding to extend our programming code to deal with more realistic inter-atomic potentials, and plan to examine the effect of the pairing interaction in the HFB framework.

VII. ACKNOWLEDGMENT

This work is supported by EPSRC with a grant EP/C520521/1.

- [1] A. Griesmaier, J. Werner, S. Hensler, J. Stuhler, T. Pfau, Phys. Rev. Lett. **94** 160401 (2005)
- [2] N. R. Cooper, E. H. Rezayi, S. H. Simon, Phys. Rev. Lett. **95** 200402 (2005)
- [3] J. Zhang, H. Zhai, Phys. Rev. Lett. **95** 200403 (2005)
- [4] M. W. Zwierlein, J. R. Abo-Shaeer, A. Schirotzek, C. H. Schunck, W. Ketterle, Nature **435** 1047 (2005)
- [5] K. W. Madison, F. Chevy, W. Wohlleben, J. Dalibard, Phys. Rev. Lett. **84** 806 (2000)
- [6] G. M. Kavoulakis, B. Mottelson, C. J. Pethick, Phys. Rev. A **62** 063605 (2000)
- [7] K. W. Madison, F. Chevy, W. Wohlleben, J. Dalibard, J. Mod. Opt. **47** 2715 (2000)
- [8] K. Kasamatsu, M. Tsubota, M. Ueda, Phys. Rev. A **67** 033610 (2003)

- [9] E. Hodby, S. A. Hopkins, G. Hechenblaikner, N. L. Smith, C. J. Foot, Phys. Rev. Lett. **91** 090403 (2003)
- [10] N. L. Smith, W. H. Heathcote, J. M. Krueger, C. J. Foot, Phys. Rev. Lett. **93** 080406 (2004)
- [11] P. Rosenbusch, V. Bretin, J. Dalibard, Phys. Rev. Lett. **89** 200403 (2002)
- [12] I. Danaila, Phys. Rev. A **72** 013605 (2005), J. J. García-Ripoll, V. M. Pèrez-García, Phys. Rev. A **64** 053611 (2001)
- [13] A. Aftalion, I. Danaila, Phys. Rev. A **68** 023603 (2003)
- [14] L.-C. Crasovan, V. M. Pèrez-García, I. Danaila, D. Mihalache, L. Torner, Phys Rev A **70** 033605 (2004)
- [15] K. Kasamatsu, M. Machida, N. Sasa, M. Tsubota Phys. Rev. A **71** 063616 (2005)
- [16] S. Komineas, N. R. Cooper, N. Papanicolaou, Phys. Rev. A **72** 053624 (2005)
- [17] M. Kumakura, T. Hirotani, M. Okano, Y. Takahashi, T. Yabuzaki Phys. Rev. A. **73** 063605 (2006)
- [18] Y. Shin, M. Saba, M. Vengalattore, T. A. Pasquini, C. Sanner, A. E. Leanhardt, M. Prentiss, D. E. Pritchard, and W. Ketterle, Phys. Rev. Lett. **93** 160406 (1998)
- [19] T. Horibata, N. Onishi, Nucl. Phys. A **596** 251 (1996)
- [20] M. Oi and P. M. Walker, Phys. Lett. B **576** 75 (2003)
- [21] A. Bohr, B. Mottelson, *Nuclear Structure* Vol. II, Benjamin (1975)
- [22] B. Mottelson, Phys. Rev. Lett. **83** 2695 (1999)
- [23] A. D. Jackson, G. M. Kavoulakis, B. Mottelson, S. M. Reimann, Phys. Rev. Lett. **86** 945 (2001)
- [24] P. Ring, P. Schuck, *The Nuclear Many-Body Problem* Springer-Verlag (1980)
- [25] G. F. Bertsch, T. Papenbrock, Phys. Rev. Lett. **83** 5412 (1999)
- [26] T. Papenbrock, G. F. Bertsch, Phys. Rev. A **63** 023616 (2001)
- [27] T. Nakajima, M. Ueda, Phys. Rev. Lett. **91** 140401 (2003)
- [28] N. N. Bogoliubov, Nuovo cimento **7** 794 (1958)
- [29] J. G. Valatin, Nuovo cimento **7** 843 (1958)
- [30] D. J. Thouless, Nucl. Phys. A **21** 225 (1960)
- [31] N. Onishi, Nucl. Phys. A **456** 279 (1986)
- [32] R. Onofrio, D. S. Durfee, C. Raman, M. Köhl, C. E. Kuklewicz, W. Ketterle, Phys. Rev. Lett. **84** 810 (2000)

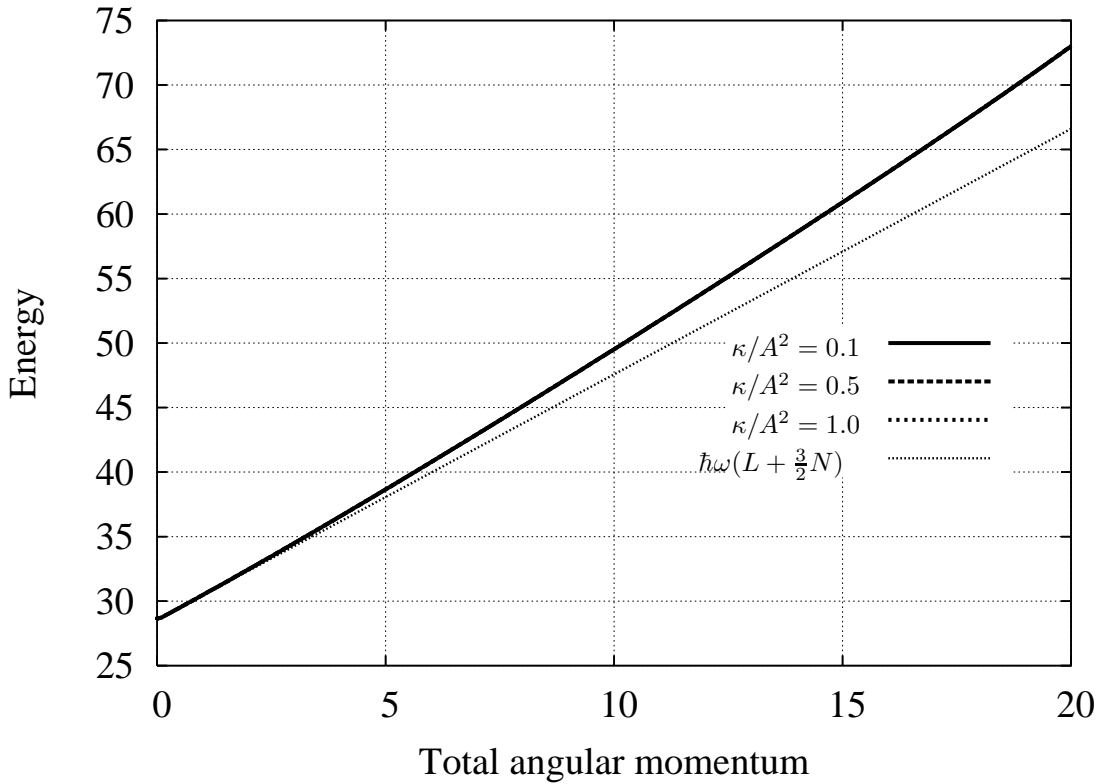


FIG. 1: The total energy (meV) as a function of the total angular momentum for $\kappa/A^2 = 0.1, 0.5$ and 1.0 (meV/ μm^4).

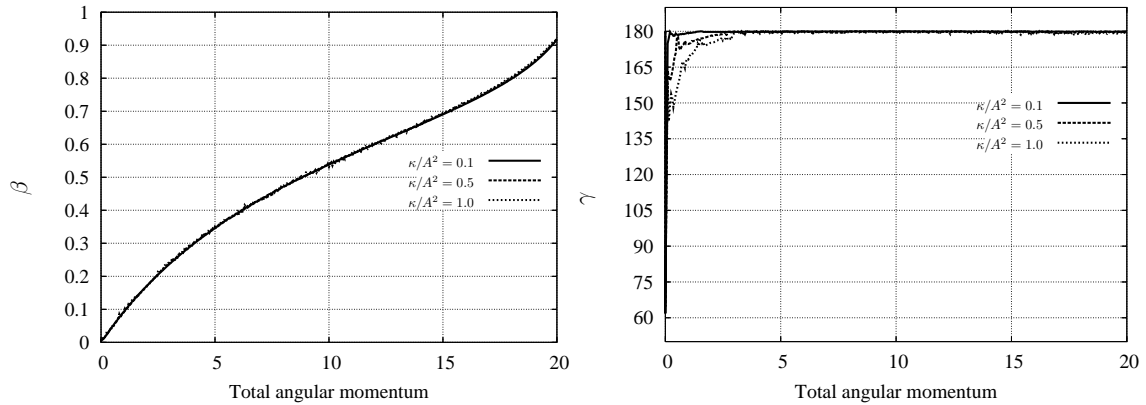


FIG. 2: The left and right panels represent the deformation parameters β (unit-less) and γ (degree) as a function of the total angular momentum, respectively.

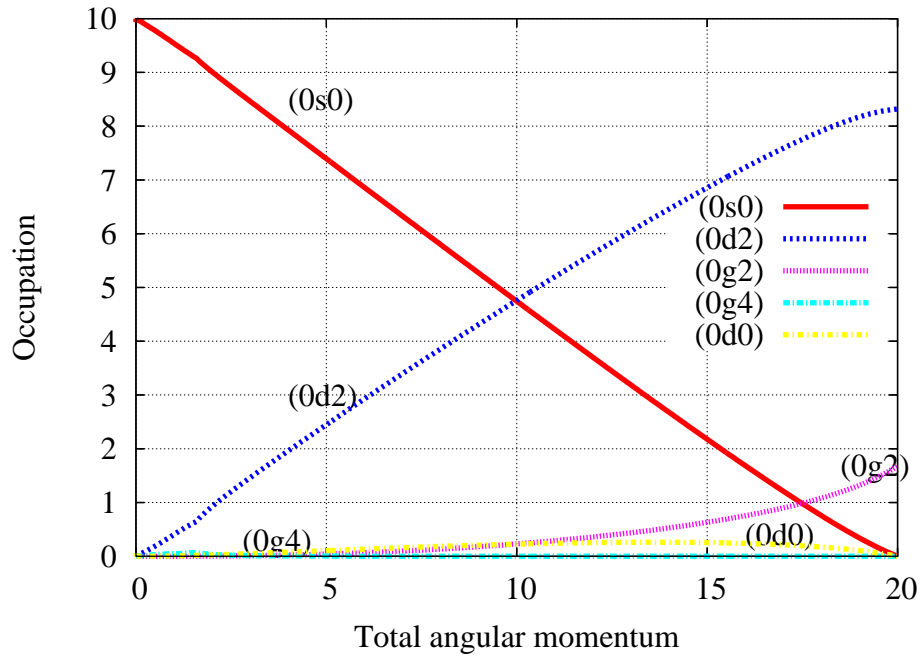


FIG. 3: (Color online) The occupation number $\rho_{\alpha\alpha}$ of the wave-function for $\kappa/A^2 = 0.1$ (meV/ μm^4). The numbers in the figure $(n_\alpha l_\alpha m_\alpha)$ stand for the principal, orbital and magnetic quantum numbers of the harmonic oscillator state.

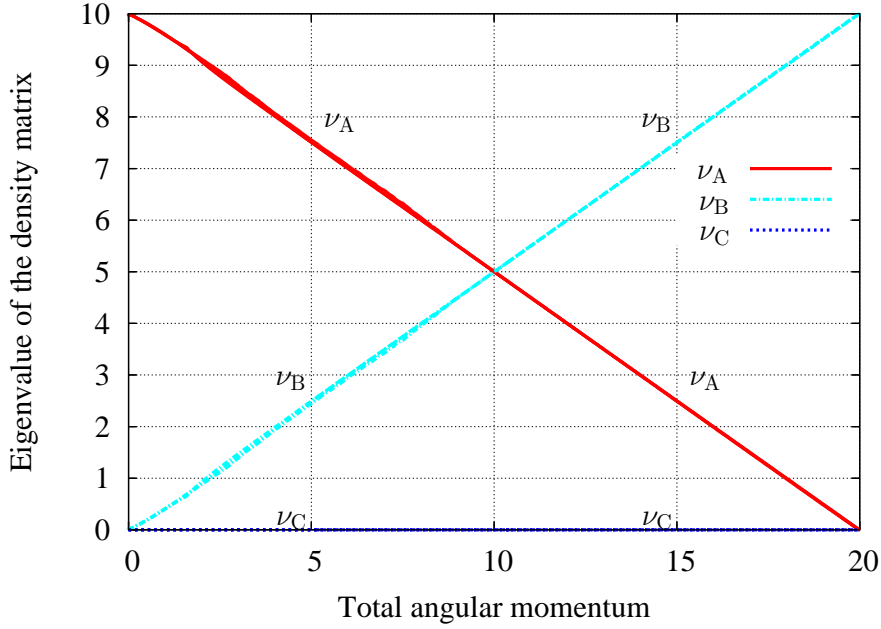


FIG. 4: (Color online) The eigenvalue ν_a of the density matrix $\rho_{\alpha\beta}$ for $\kappa/A^2 = 0.1$ (meV/ μm^4) as a function of the total angular momentum. Only the three eigenvalues ν_A, ν_B, ν_C are plotted because the other eigenvalues are almost zero.

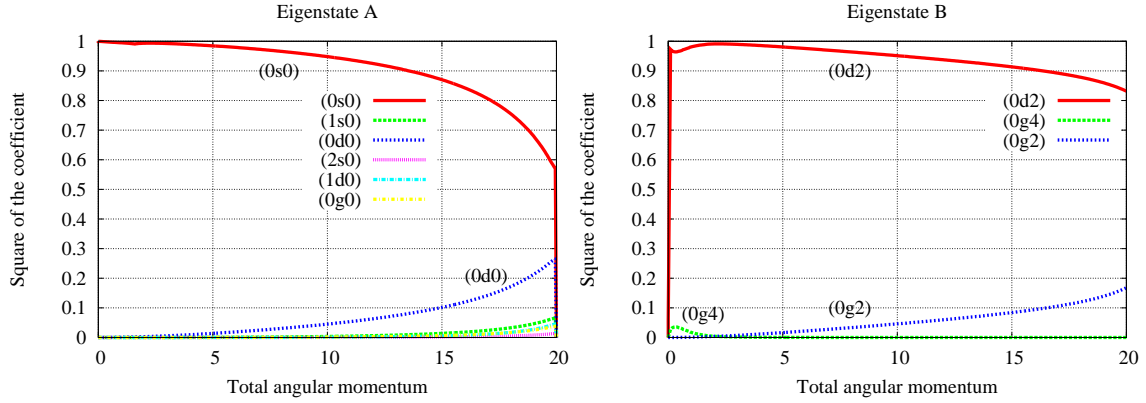


FIG. 5: (Color online) Left (right) panel represents the components for eigenstate ψ^A (ψ^B) of the density matrix as a function of the total angular momentum, respectively. The eigenstate ψ^A (ψ^B) corresponds to the eigenvalue ν_A (ν_B) in Figure 4.